Liquiritigenin inhibits hepatic fibrogenesis and TGF-β1/Smad with Hippo/Yap signal

Eun Hye Lee , Kwang-Il Park , Kwang-Youn Kim , Ju-Hee Lee , Eun Jeong Jang , Sae Kwang Ku , Sang Chan Kim , Ho Young Suk , Ji Young Park , Su Youn Baek , Young Woo Kim

PII: S0944-7113(18)30597-X
DOI: https://doi.org/10.1016/j.phymed.2018.12.003
Reference: PHYMED 52780

To appear in: *Phytomedicine*

Received date: 18 April 2018
Revised date: 23 November 2018
Accepted date: 9 December 2018

Please cite this article as: Eun Hye Lee , Kwang-Il Park , Kwang-Youn Kim , Ju-Hee Lee , Eun Jeong Jang , Sae Kwang Ku , Sang Chan Kim , Ho Young Suk , Ji Young Park , Su Youn Baek , Young Woo Kim , Liquiritigenin inhibits hepatic fibrogenesis and TGF-β1/Smad with Hippo/Yap signal, *Phytomedicine* (2018), doi: https://doi.org/10.1016/j.phymed.2018.12.003

Liquiritigenin inhibits hepatic fibrogenesis and TGF-β1/Smad with Hippo/Yap signal

Eun Hye Lee[b,#], Kwang-Il Park[c,#], Kwang-Youn Kim[c,#], Ju-Hee Lee[d], Eun Jeong Jang[a], Sae Kwang Ku[a], Sang Chan Kim[a], Ho Young Suk[e], Ji Young Park[b], Su Youn Baek[a,*], Young Woo Kim[a,*]

[a] College of Oriental Medicine, Daegu Haany University, Gyeongsan 38610, Korea

[b]Department of Pathology, School of Medical Science, Kyungpook National University, Daegu 41566, Korea

[c] Korea Institute of Oriental Medicine, Daegu 41062, Korea

[d] College of Korean Medicine, Dongguk University, Gyeongju, 38066 Korea

[e] Yeungnam University, Gyeongsan 38541, Korea

*Correspondence authors: Dr. YW Kim, E-mail: ywkim@dhu.ac.kr; Dr. SY Baek, E-mail: rhodeus@dhu.ac.kr, College of Oriental Medicine, Daegu Haany University, Gyeongsan, 38610, Korea. Fax: +82-53-819-1860, Tel: +82-53-819-1867

#These authors equally contributed to this work.

Running title: Liquiritigenin inhibits liver fibrosis

Abstract

Backgroud: Recent reports highlighted the possibility that Yes-associated protein (Yap) and transforming growth factor-β1 (TGF-β1) can act as critical regulators of hepatic stellate cells (HSCs) activation; therefore, it is natural for compounds targeting Hippo/Yap and TGF-β1/Smad signaling pathways to be identified as potential anti-fibrotic candidates.

Purpose: Liquiritigenin (LQ) is an aglycone of liquiritin and has been reported to protect the liver from injury. However, its effects on the Hippo/Yap and TGF-β1/Smad pathways have not been identified to date.

Methods: We conducted a series of experiments using CCl_4-induced fibrotic mice and cultured LX-2 cells.

Result: LQ significantly inhibited liver fibrosis, as indicated by decreases in regions of hepatic degeneration, inflammatory cell infiltration, and the intensity of α-smooth muscle actin (α-SMA) staining in mice. Moreover, LQ blocked the TGF-β1-induced phosphorylation of Smad 3, and the transcript levels of plasminogen activator inhibitor-1 (PAI-1) and matrix metalloproteinase-2 (MMP-2) in LX-2 cells, which is similar with resveratrol and oxyresveratrol (positive controls). Furthermore, LQ increased activation of large tumor suppressor kinase 1 (LATS1) with the induction of YAP phosphorylation, thereby preventing YAP transcriptional activity and suppressing the expression of exacerbated TGF-β1/Smad signaling molecules.

Conclusion: These results clearly show that LQ ameliorated experimental liver fibrosis by acting on the TGF-β1/Smad and Hippo/Yap pathways, indicating that LQ has the potential for effective treatment of liver fibrosis.

Key words: Liquiritigenin; liver; fibrosis; Hippo/YAP; TGF-β1/Smad

Abbreviations: α-SMA, α-smooth muscle actin; ALT, alanine aminotransferase; APAP, acetaminophen; CCl4, carbon tetrachloride; CTGF, connective tissue growth factor; ECM, extracellular matrix; H&E, hematoxylin and eosin; HCC, hepatocellular carcinoma; HNE, hydroxynonenal; HO, heme oxygenase ; HSC, hepatic stellate cells; LATS1, Large Tumor Suppressor Kinase 1; LQ, Liquiritigenin; PAI, plasminogen activator inhibitor; PDGF, platelet-derived growth factor; TGF, transforming growth factor; TNF, tumor necrosis factor; ROS, reactive oxygen species; PGC, peroxisome proliferator-activated receptor-gamma coactivator; SMA, smooth muscle actin; SPP, secreted phosphate protein; YAP, Yes-associated protein

Introduction

Liquiritigenin (LQ) is an aglycone of liquiritin in licorice, and has been shown to have various pharmacological activities including antioxidant, anti-inflammatory, anti-tumor, and anti-diabetic activities (Gaur et al., 2014; Kim et al., 2008; Wang et al., 2014). A number of studies have demonstrated that LQ plays a role in the liver as a hepatic protectant. LQ exerts cytoprotective effects against heavy metals-induced toxicity *in vitro* as well as against acute liver injuries induced by acetaminophen (APAP) *in vivo* (Kim et al., 2004; Kim et al., 2006). LQ has also been shown to induce the secretion of bile by induction of antioxidant phase-II enzymes (Kim et al., 2009), as well as to exert protective effects against liver injuries via the PGC-1α pathway (Zhang et al., 2015). However, no detailed molecular evidence of the effects of LQ on the liver fibrogenesis and TGF-β1/Smad pathways has been provided to date.

Liver fibrosis is a wound-healing process caused by most types of chronic damage to the liver, including alcohol abuse, hepatitis virus infection, biliary obstruction, and nonalcoholic fatty liver disease (Bataller and Brenner, 2005; Friedman, 2008; Ramachandran and Iredale, 2012). Fibrosis is normally characterized by the accumulation of extracellular matrix (ECM) proteins, which form fibrous scars and develop nodules, distorting the hepatic architecture. If fibrogenesis persists, cirrhosis may develop and the risk of developing hepatocellular carcinoma (HCC) increases (Friedman, 2008; Sakurai and Kudo, 2013).

Activation of hepatic stellate cells (HSCs) has been recognized as an important component during the initiation and development of liver fibrosis (Puche et al., 2014). In normal livers, the quiescent HSCs reside in the space known as the Disse and store retinoids. However, upon liver injury, HSCs are activated to undergo a transition to contractile, matrix-producing myofibroblasts. The transition to myofibroblasts, in turn, induces gene

transcription of fibrillar collagen and α-smooth muscle actin (α-SMA), leading to formation of stress fiber, deposition of extracellular matrix and enlarged cell-extracellular matrix contact (Higashi et al., 2017; Puche et al., 2014). Thus, elucidating the molecular mechanisms that trigger HSC activation is the most important part of regulating fibrotic responses.

The TGF-β1/Smad signaling is known to play a critical role in activation of HSCs and regulation of the production and accumulation of ECM proteins (Fabregat et al., 2016). The onset of TGF-β1/Smad signaling occurs when TGF-β binds to the serine/threonine kinase receptor, TβRII, phosphorylating its transducer receptor, TβRI. The activated TβRI then recruits and phosphorylates R-Smads (Smad2/3), which are transcription factors that typically bind co-Smad (Smad4), after which these R-Smad complexes accumulate in the cell nucleus, where they increase the transcriptional level of specific target genes (e.g., collagen-I) (Inagaki and Okazaki, 2007).

Recent studies suggested that the Hippo pathway and its downstream effector, Yes-associated protein (YAP), act as critical regulators of HSC activation (Mannaerts et al., 2015). In recent studies, YAP was found to be elevated in the nucleus through HSC activation and the inhibition of YAP prevented early HSC activation *in vitro* as well as the overall processes of fibrogenesis *in vivo* (Mannaerts et al., 2015). Therefore, the present study investigated the mechanistic action of LQ on the Hippo/Yap and TGF-β1/Smad pathways in liver fibrogenesis associated with HSCs activation using an *in vivo* mouse model of liver fibrosis induced by carbon tetrachloride (CCl_4) and an *in vitro* model based on LX-2 cells treated with or without TGF-β1.

Materials and Methods

Materials

LQ was isolated from *Glycyrrhizae radix* (Sejong, Daegu, Korea) warranted as a standard herb for medicine by Korea Food and Drug Administration (Ref. No. GLUR2008). Isolation of the compound was verified by a series of spectroscopic analyses by Dr. Jong-Rok Lee (Daegu Haany University) as previously described (Kim et al., 2006)(figure 1). Briefly, *G. radix* (3 kg) was extracted with 15 L methanol for 72 h, and this extracts were concentrated to make a dark gum. The fraction of CHCl3–MeOH was concentrated to produce an additional residue, and these were evaporated to have a liquiritin-rich fraction, which were moved to silica gel CC to obtain liquiritin. And then, LQ was prepared by acid hydrolysis of this liquiritin. Briefly, liquiritin was reconstituted in DMSO and with 0.1N HCl, all of which were heated at 100 ◦C. Conversion of liquiritin to LQ was verified by HPLC and NMR analyses. The hydrolysate was solved with 40% methanol and analyzed by HPLC using an H-80 column (250 mm×10 mm). The amount of LQ was quantitated by monitoring absorbance at 254 nm, and the efficiency was calculated from LQ produced (>95% purity). NMR analysis also determined the authenticity of LQ. TGF β1 was purchased from R&D Systems (Minneapolis, MN, USA). Anti-p-Smad 3, anti-p-YAP, anti-p-LATS1, anti-PAI-1 and anti-β-actin antibody were supplied from Cell Signaling Technologies (Danvers, MA, USA). Anti-YAP and anti-mouse IgG kappa binding protein (m-IgGκ BP) conjugated to fluorescein (FITC) antibody were obtained from Santa Cruz Biotechnology (Santa Cruz, CA, USA). Anti-α-SMA, 3-(4,5-dimethylthiazol-2-yl)-2,5-diphenyl-tetrazolium bromide (MTT) and other reagents were purchased from Sigma–Aldrich (St. Louis, MO, USA).

Animals and experimental protocol

Animal studies were conducted in accordance with the institutional guidelines for animal experinents, and were approved by the Institutional Animal Care and Use Committee of the Daegu Haany University. To induce liver fibrosis, CCl_4 (0.5 ml/kg) dissolved in olive oil (5 %) was intraperitoneally injected into the C57BL/6 mice (male, 20 – 22 g) twice a week for 4 weeks (Lee et al., 2014). LQ, dissolved in 40% PEG 400, was orally administered (four times per week for 4 weeks) at the dose of 10 or 30 mg/kg/day (Fig. 2A), which were the effective doses to treat the hepatic oxidative damage in the previous study (Park et al., 2015). The mice were assigned into four groups, control, CCl_4, CCl_4 + LQ (lower dose) and CCl_4 +LQ (higher dose).

Blood chemistry

Serum level of alanine aminotransferase was measured based on the standard enzymatic techniques using ALT Colorimetric Activity Assay Kit (Cayman, Ann Arbor, MI, USA) according to manufacturer's instructions (Lee et al., 2014).

Histological process and immunohistochemistry

Histological analysis was performed and determined by Dr. Sae-Kwang Ku (Department Histology, College of Oriental Medicine, Daegu Haany University) as previously described (Lee et al., 2007; Lee et al., 2014). Liver were embedded in paraffin and sectioned (3 ~ 4 μm) (Lee et al., 2014). Sections were stained with hematoxylin and eosin (H&E) for general histopathology or with Masson's trichrome for collagen fibers. The expression levels of α-

SMA, nitrotyrosine, and 4-hydroxynonenal (4-HNE) were determined using the immunohistochemistry tool as previously described (Cho et al., 2010). Tissue sections were stained using avidin – biotin methods (Vector Labs., Inc.).

Histomorphometry

The percentages of collagen fiber occupied area in hepatic parenchyma, numbers of degenerative hepatocytes and numbers of inflammatory cells infiltrated were calculated using a digital image analyzer (iSolution FLver 9.1, IMT i-solution Inc., Quebec, Canada), according to our previously established methods (Lee et al., 2007; Lee et al., 2014). In addition, the effects on the α-SMA, 4-HNE and nitrotyrosine immunoreactivities were also measured using digital image analyzer in the restricted view fields of liver tissue.

Cell culture and Western blot analysis

LX-2 cells, an immortalized human HSCs line, were kindly provided by Dr. SL Friedman (Mount Sinai School of Medicine, NY, USA) (Lee et al., 2014). Cells were treated with LQ (30 and/or 100 μM). Preparation of protein lysates from cell line and liver tissue were performed as previously described protocol (Lee et al., 2014).

Real-time RT-PCR analysis

Total RNA was extracted using a Trizol (Invitrogen, Carlsbad, CA, USA)(Cho et al., 2010). Real-time PCR was performed using MG 2X qPCR mastermix (MGmed, Seoul, Korea) with a SYBR green premix, and primer sets were shown in Table 1.

Immunocytochemistry

Untreated or LQ (100 μM for 1h)-treated LX-2 cells was fixed for 10 min in 4 % paraformaldehyde at room temperature. The cells were incubated with anti-YAP antibody (1:200) for overnight, and FITC-conjugated secondary antibodies (1:200). The slides were mounted with 80 % glycerol in PBS with DAPI (0.3 μg/ml).

Data analysis

A Multiple comparison tests for different dose groups were conducted as previously described (Lee et al., 2014). Variance homogeneity was determined by using the Levene test (Levene, 1981). The statistical significance of the differences among the treatment groups was verified by one-way analysis of variance (ANOVA). An unpaired t-test was also used to analyze the differences, and a non-parametric test was used (Mann-Whitney U test) if the distribution of data was abnormal. All the statistical analyses were performed using Stat View 5.0 (Abacus Concepts, Berkeley, CA). P values were displayed with asterisks (*** ; $P < 0.001$, **; $P < 0.01$, *; $P < 0.05$, ns; $P > 0.05$).

Results

Liquiritigenin protected the liver from CCl_4-induced toxicity

CCl_4 is known to induce liver toxicity and resultantly produce highly reactive metabolites (Manibusan et al., 2007). And, a long exposure of this insult results severe hepatocyte injury and initiated pathological process of fibrosis (Manibusan et al., 2007). Repeated injections of CCl_4 (2 times/week, 4 weeks) significantly elevated the level of ALT ($P < 0.01$). However, the level was attenuated by oral administration of two concentrations of LQ (10 mg/kg and 30 mg/kg; both $P < 0.05$)(Fig. 2A). Histopathological analysis showed that CCl_4 treatment induced the ballooning of hepatocytes and the infiltration of inflammatory cells in the liver tissue (Fig. 2B). The number of degenerative hepatocytes as well as the number of inflammatory cells was markedly increased in the CCl_4 treated mice (Table 2). However, LQ protected these kinds of hepatic damage (Fig. 1B and Table 2).

Liquiritigenin ameliorates CCl_4-induced liver fibrosis

To examine the potential effects of LQ on collagen occupation during fibrosis, the tissues were stained with α-SMA and Masson's trichrome. α-SMA-immunolabeled cells were significantly ($P < 0.01$) increased in the central vein regions in response to CCl_4 treatment (Fig. 3A). These CCl_4 treatment-related increases of α-SMA immunoreactivities in hepatic parenchyma were dose-dependently inhibited by treatment with LQ (Fig. 3B). Moreover, CCl_4 markedly induced collagen fibers, as indicated with fibrotic septa between each nodule, which were significantly decreased by LQ treatment (Fig. 3B). Moreover, the collagen fiber occupied percentages in the CCl_4-treated group increased significantly when compared with

the vehicle control, while they were attenuated in both LQ 10 and 30 mg/kg treated mouse livers (data not shown).

Because oxidative stress was believed to be an important mediator of liver fibrosis (Sánchez-Valle et al., 2012), additional analyses were performed to examine whether LQ could inhibit oxidative stress in CCl_4-induced liver fibrosis. The numbers of nitrotyrosine or 4-HNE-positive cells in the CCl_4 control were increased relative to the intact control, whereas the level was attenuated in response to treatment with LQ (Fig. 3C).

Liquiritigenin suppressed TGF-β1/Smad signaling and HSC activation in vitro

To study the mechanisms of LQ inhibition of hepatic fibrosis *in vivo*, we conducted *in vitro* studies using LX-2 cells, a human HSC cell line. Before examination, we tested the cytotoxicity of LQ in LX-2 cells. MTT assay showed no significant differences in LX-2 cells treated with LQ 100 μM (Supplementary Fig. S1). Therefore, we used concentrations of 30 μM (lower effect) and 100 μM (higher effect).

The TGF-β1-mediated signaling pathway is known to mediated with the phosphorylation of Smad 2/3 (Inagaki and Okazaki, 2007). To reveal the underlying mechanisms responsible for the inhibition of HSCs activation, authors determined the effects of the compound on signal transduction of TGF-β/Smad. As expected, TGF-β1 enhanced α-SMA levels, but this was inhibited by LQ pretreatment (Fig. 4A). Real-time-PCR analysis showed that the LQ markedly suppressed the TGF-β1-induced gene expression of PAI-1 and MMP-2 (Fig. 4B). Moreover, LQ also inhibited autophagy-related protein induction (i.e. LC3-II) by TGF-β1 (Fig. 4C).

Next, we determined signaling pathway of Smad. Smad proteins are of great importance

in the progression of fibrosis. Smad3 is related with R-Smad, the representative in three subtype of Smads, which also include Co-Smad (Smad4) and I-Smad (Smad 7). Immunoblot analysis revealed an increase in the Smad3 phosphorylation by TGF-β1, as well as inhibition of this increase by LQ treatment (Fig. 5A). Moreover, LQ inhibited dysregulation of Smad4 and 7 induced by TGF-β1 (Fig. 5B). As a positive control experiment, resveratrol and oxyresveratrol also inhibited the Smad3 activation and α-SMA as similar with LQ (Fig. 5C).

Liquiritigenin activated hippo signaling

Recently, YAP has been shown to play essential roles in liver cell fate and HSC activation. YAP activity is regulated by phosphorylation, which causes YAP inactivation and nuclear to cytoplasmic translocation (Mannaerts et al., 2015; Meng et al., 2016). To examine the time course of the effects of LQ on the hippo signaling pathway, we treated LX-2 cells with 100 μM LQ. The level of phospho LATS1, a negative regulator of YAP, increased after treatment with LQ for 0.5 –3 h. In addition, the phosphorylation level of YAP was robustly elevated 1 h after treatment with LQ at 100 μM (Fig. 6A). To verify the effects of LQ on the hippo signaling pathway, the levels of Yap were measured by immunocytochemistry analysis (Fig. 5B). In the vehicle control (LX-2 cells) the Yap signal was low and mostly located in the nucleus (Fig. 6B). In comparison, Yap was robustly expressed with high amounts present in the cytoplasm of LQ treated LX-2 cells (Fig. 6B). Moreover, we tested the effect of verteporfin, a chemical inhibitor of YAP. As expected, the treatment of verteporfin (0.4 μM) inhibited TGF-b1-induced α-SMA, and co-treatment of LQ and verteporfin attenuated the expression of α-SMA more than LQ alone (Fig. 6C).

We next tested whether LQ could affect YAP signaling in fibrogenesis *in vivo*. Both the

phosphorylated form of YAP and LATS1 were significantly decreased in the CCl_4-induced fibrotic group compared to the control group (Fig. 7A). However, LQ treatment of the CCl_4-induced group led to increase them relative to CCl_4-induced mice (Fig. 7A), indicating that LQ has profound effects on YAP activity and HSC activation. Collectively, these results suggest that LQ activates the hippo signaling pathway, which might contribute LQ's protection against liver fibrosis (Fig. 7B).

Discussion

Here, we investigated the efficiency of LQ as a candidate for hepatic fibrosis control and attempted to examine its functional mechanism across a series of experimental tests. Hepatic fibrosis was induced using carbon tetrachloride (CCl_4), a representative hepatotoxic substance (Manibusan et al., 2007; Yazdani et al., 2017). When CCl_4 enters the hepatocytes, it is converted to CCl_3 by cytochrome P450 (CYP450) located in the smooth endoplasmic reticulum. Both CCl_3 and CCl_3O_2, which are created by binding with intracellular oxygen, are highly reactive, resulting in damage to various cellular functions, such as destruction of the endogenous reticulum or disruption of mitochondrial and intracellular enzyme activities, which ultimately leads to the development of cirrhosis, usually after 4 to 8 weeks (Lee et al., 2014; Manibusan et al., 2007). As predicted, we observed significant liver damage in the experimental mice subjected to intraperitoneal injection of CCl_4 for 4 weeks. However, treatment with CCl_4 in the presence of LQ resulted in a marked decrease in local fibrosis and α-SMA expression, as well as pathological histologic liver damage such as increased CCl_4-induced ALT activity, inflammation and necrosis. Moreover, these effects occurred in a dose dependent manner, indicating its beneficial effects at protecting the liver from damage and the gene expression of liver fibrosis. The results of these *in vivo* experiments support those of previous studies showing that LQ has protective effects on hepatocyte injury induced by heavy metals or liver damage induced by acetaminophen (Kim et al., 2004; Kim et al., 2006). Moreover, LQ has been known to be metabolized to glucuronide conjugates (Kim et al., 2009). In our previous finding, the time profiles of LQ and its metabolites showed that the contents of metabolites rapidly increased after treatment and remained for a long time (Kim

et al., 2009). However, it needs to clarify the exact pharmacokinetic profile to arrange the time schedule and oral dose in the chronic disease model.

The increased number of nitrotyrosine- or 4-HNE-positive cells by CCl_4 injections was attenuated by LQ treatments, indicating that oxidative stress can also be alleviated in the fibrous liver by LQ. Oxidative stress is known to induce the synthesis of inflammatory cytokines and modulates HSC activation (Sánchez-Valle et al., 2012). Thus, ROS is an important initiator and amplifier during pathological progress of fibrosis in the liver (Sánchez-Valle et al., 2012; Seki and Schwabe, 2015). Our results clearly support those of a previous report showing that LQ plays an important role in mitigating CCl4-induced liver damage by regulating PGC-1α and its downstream genes (Zhang et al., 2015). Taken together, the results of our study showed that LQ can inhibit hepatic damage and HSC activation caused by oxidative stress and eventually liver fibrosis.

Inflammatory reactions caused by hepatocyte injury stimulate liver parenchymal cells, endothelial cells, or Kupffer cells to release various cytokines and chemokines. Among these, TGF-β1 is known to act as a key factor in liver fibrosis (Fabregat et al., 2016; Friedman, 2008). Upon activation of TGF-β1, HSCs are transformed into myofibroblast-like form and rapidly proliferate to over-synthesize ECM proteins such as collagen, proteoglycan, and fibronectin for the establishment of connective tissues, thereby promoting liver fibrosis (Cho et al., 2010). In addition, TGF-β1 inhibits the degradation of ECM by regulating matrix metalloproteinase (MMP), tissue inhibitors of metalloproteinases (TIMP), which inhibits MMP, and plasminogen activator inhibitor (PAI) (Dudás et al., 2001). TGF-β expression is also known to be associated with progressive liver disease (Friedman, 2008; Lee and Friedman, 2011).

The standard TGF-β signaling pathway is the TGF-β1/Smad signaling pathway, in which TGF-β1 binds to receptors present on the plasma membrane to activate the Smad signaling pathway, thereby increasing the level of procollagen, the collagen precursor, and transcription of the downstream genes (Moustakas and Heldin, 2009). Our results showed that LQ inhibited Smad3 phosphorylation and activation by TGF-β1, subsequently blocking fibrotic gene expression in HSCs (Fig. 4), suggesting that the effects of LQ on liver fibrosis are at least partly related to regulation of the TGF-β1/Smad signaling pathway.

Recent studies have demonstrated that the YAP protein in the Hippo signaling pathway plays a key role in the activation of HSCs. One study showed that Yap was involved in the progression of fibrosis with HSC activation in mice treated with CCl_4. This was further confirmed by the additional experimental results that showed expression of α-SMA and collagen-1 was drastically reduced and not activated when Yap was completely knocked down (Mannaerts et al., 2015). Activation of HSCs leads to overproduction of ECM, which can be used to protect damaged tissues and appears to involve YAP. The function of YAP as a sensor of stress and a driver of regeneration processes was observed not only in HSCs, but also other types of cells and organs. For example, a study showed that YAP expression in epithelial cells of the intestinal crypt was increased in response to toxin-induced tissue damage, and that lack of YAP would make it impossible to regenerate damaged intestinal tissue (Barry et al., 2012, Zhubanchaliyev et al., 2016). YAP overexpression in the heart with ischemic injury promotes cardiac muscle regeneration, indicating that YAP is associated with wound healing (Del Re et al., 2013; Xin et al., 2013). In addition, fibroblasts expressing activated YAP have been found to promote fibrosis when implanted into the lungs of rats (Liu et al., 2015). Overall, YAP activation appears to play a decisive role in causing fibroblast

responses *in vivo*.

The YAP/TAZ of the Hippo signaling pathway interacts with TGF-β-induced Smad2/3 in the nucleus, resulting in a YAP/TAZ•TEAD•Smad2/3 complex, which regulates several transcription processes induced by TGF-β (Grannas et al., 2015; Nishio et al., 2016; Varelas et al., 2010). Activation of the Hippo signaling pathway results in phosphorylation of YAP, which causes it to remain in the cytoplasm. However, when the Hippo signaling pathway is inactivated, it migrates to the nucleus and interacts with the TEAD1-4 transcription factor, promoting transcription of genes such as CTGF, SPP1 and TGF-β (Perumal et al., 2017; Zhao et al., 2008). Therefore, we investigated whether LQ induces phosphorylation of YAP protein. Liquiritigenin treatment was found to induce phosphorylation of YAP protein in LX-2 cells and in mice bearing CCl_4-induced liver fibrosis. Immunocytochemistry analysis revealed that phosphorylation of YAP was significantly increased in LX-2 cells treated with LQ, and it was clearly observed in the cytoplasm, indicating that YAP was inactivated. In summary, LQ induced phosphorylation of YAP, which inhibited activation of YAP/TAZ, thereby ultimately blocking HSC activation and TGF-β1/Smad signaling.

Conclusion

The results of our study clearly indicate that LQ significantly inhibited liver fibrosis in mouse models *in vivo* and HSC activation *in vitro*. This protective mechanism might be related to its ability to hippo signaling and the TGF-β1/Smad signaling pathway. Based on these findings, LQ is expected to play a beneficial role in the treatment of liver fibrosis and chronic liver disease.

Conflict of interest

The authors declare that there are no conflicts of interest

Acknowledgements

This work was supported by the National Research Foundation of Korea (NRF) grant funded by the Korea Government [MSIP] (No. 2017R1D1A3B03027847), and also by the grant K18102 awarded to Korea Institute of Oriental Medicine (KIOM) from Korea Ministry of Education, Science and Technology (MEST). Lee EH would like to thank to the Ph.D.'s program of Kyungpook National University for completing the Ph.D. thesis through this work (Academic advisor: Dr. Ji Young Park). Authors appreciate Dr. Jong-Rok Lee (Daegu Haany University) for the isolation of liquiritigenin from *Glycyrrhizae radix*, and the laboratory of Dr. Sae Kwang Ku (Daegu Haany University) for histological analysis.

References

Barry, E.R., Morikawa, T., Butler, B.L., Shrestha, K., de la Rosa, R., Yan, K.S., Fuchs, C.S., Magness, S.T., Smits, R., Ogino, S., Kuo, C.J., Camargo, F.D., 2012. Restriction of intestinal stem cell expansion and the regenerative response by YAP. Nature 493(7430), 106-10. http://dx.doi.org/10.1038/nature11693

Bataller, R., Brenner, D.A., 2005. Liver fibrosis. J. Clin. Invest. 15(2), 209-18. http://dx.doi.org/10.1172/JCI24282

Cho, I.J., Kim, Y.W., Han, C.Y., Kim, E.H., Anderson, R.A., Lee, Y.S., Lee, C.H., Hwang, S.J., Kim, S.G., 2010. E-cadherin antagonizes transforming growth factor β1 gene induction in hepatic stellate cells by inhibiting RhoA-dependent Smad3 phosphorylation. Hepatology 52(6), 2053-64. http://dx.doi.org/10.1002/hep.23931

Del Re, D.P., Yang, Y., Nakano, N., Cho, J., Zhai, P., Yamamoto, T., Zhang, N., Yabuta, N., Nojima, H., Pan, D., Sadoshima, J., 2013. Yes-associated protein isoform 1 (Yap1) promotes cardiomyocyte survival and growth to protect against myocardial ischemic injury. J. Biol. Chem. 288(6), 3977-88. http://dx.doi.org/10.1074/jbc.M112.436311

Dudás, J., Kovalszky, I., Gallai, M., Nagy, J.O., Schaff, Z., Knittel, T., Mehde, M., Neubauer, K., Szalay, F., Ramadori, G., 2001. Expression of decorin, transforming growth factor-beta 1, tissue inhibitor metalloproteinase 1 and 2, and type IV collagenases in chronic hepatitis. Am. J. Clin. Pathol. 115(5), 725-35. http://dx.doi.org/10.1309/J8CD-E9C8-X4NG-GTVG

Fabregat, I., Moreno-Càceres, J., Sánchez, A., Dooley, S., Dewidar, B., Giannelli, G., Ten Dijke, P.; IT-LIVER Consortium, 2016. TGF-β signalling and liver disease. FEBS J. 283(12), 2219-32. http://dx.doi.org/10.1111/febs.13665

Friedman, S.L., 2008. Mechanisms of hepatic fibrogenesis. Gastroenterology 134(6), 1655-69. http://dx.doi.org/10.1053/j.gastro.2008.03.003

Gaur, R., Yadav, K.S., Verma, R.K., Yadav, N.P., Bhakuni, R.S., 2014. In vivo anti-diabetic activity of derivatives of isoliquiritigenin and liquiritigenin. Phytomedicine 21(4), 415-22. http://dx.doi.org/10.1016/j.phymed.2013.10.015

Grannas, K., Arngården, L., Lönn, P., Mazurkiewicz, M., Blokzijl, A., Zieba, A., Söderberg, O., 2015. Crosstalk between Hippo and TGFβ: Subcellular Localization of YAP/TAZ/Smad Complexes. J. Mol. Biol. 427(21), 3407-15. http://dx.doi.org/10.1016/j.jmb.2015.04.015

Higashi, T., Friedman, S.L., Hoshida, Y., 2017. Hepatic stellate cells as key target in liver fibrosis. Adv. Drug Deliv. Rev. 121, 27-42. http://dx.doi.org/10.1016/j.addr.2017.05.007

Inagaki, Y., Okazaki, I., 2007. Emerging insights into transforming growth factor beta Smad signal in hepatic fibrogenesis. Gut 56(2), 284-92. http://dx.doi.org/10.1136/gut.2005.088690

Kim, S.C., Byun, S.H., Yang, C.H., Kim, C.Y., Kim, J.W., Kim, S.G., 2004. Cytoprotective effects of *Glycyrrhizae radix* extract and its active component liquiritigenin against cadmium-induced toxicity (effects on bad translocation and cytochrome c-mediated PARP cleavage). Toxicology 197(3), 239-51. http://dx.doi.org/10.1016/j.tox.2004.01.010

Kim, Y.W., Kang, H.E., Lee, M.G., Hwang, S.J., Kim, S.C., Lee, C.H., Kim, S.G., 2009. Liquiritigenin, a flavonoid aglycone from licorice, has a choleretic effect and the ability to induce hepatic transporters and phase-II enzymes. Am. J. Physiol. Gastrointest. Liver Physiol. 296(2), G372-81. http://dx.doi.org/10.1152/ajpgi.90524.2008

Kim, Y.W., Ki, S.H., Lee, J.R., Lee, S.J., Kim, C.W., Kim, S.C., Kim, S.G., 2006.

Liquiritigenin, an aglycone of liquiritin in *Glycyrrhizae radix*, prevents acute liver injuries in rats induced by acetaminophen with or without buthionine sulfoximine. Chem. Biol. Interact. 161(2), 125-38. http://dx.doi.org/10.1016/j.cbi.2006.03.008

Kim, Y.W., Zhao, R.J., Park, S.J., Lee, J.R., Cho, I.J., Yang, C.H., Kim, S.G., Kim, S.C., 2008. Anti-inflammatory effects of liquiritigenin as a consequence of the inhibition of NF-kappaB-dependent iNOS and proinflammatory cytokines production. Br. J. Pharmacol. 154(1), 165-73. http://dx.doi.org/10.1038/bjp.2008.79

Lee, H.S., Keum, K.Y., Ku, S.K.., 2007. Effects of *Picrorrhiza rhizoma* water extracts on the subacute liver damages induced by carbon tetrachloride. J. Med. Food. 10(1), 110-7. http://dx.doi.org/10.1089/jmf.2006.0114

Lee, J.H., Jang, E.J., Seo, H.L., Ku, S.K., Lee, J.R., Shin, S.S., Park, S.D., Kim, S.C., Kim, Y.W., 2014. Sauchinone attenuates liver fibrosis and hepatic stellate cell activation through TGF-β/Smad signaling pathway. Chem. Biol. Interact. 224, 58-67. http://dx.doi.org/10.1016/j.cbi.2014.10.005

Lee, U.E., Friedman, S.L., 2011. Mechanisms of hepatic fibrogenesis. Best Pract. Res. Clin. Gastroenterol. 25(2), 195-206. http://dx.doi.org/10.1016/j.bpg.2011.02.005

Levene, A., 1981. Pathological factors influencing excision of tumours in the head and neck. Part I. Clin. Otolaryngol. Allied Sci. 6(2), 145-51

Liu, F., Lagares, D., Choi, K.M., Stopfer, L., Marinković, A., Vrbanac, V., Probst, C.K., Hiemer, S.E., Sisson, T.H., Horowitz, J.C., Rosas, I.O., Fredenburgh, L.E., Feghali-Bostwick, C., Varelas, X., Tager, A.M., Tschumperlin, D.J., 2015. Mechanosignaling through YAP and TAZ drives fibroblast activation and fibrosis. Am. J. Physiol. Lung Cell Mol. Physiol. 308(4), L344-57. http://dx.doi.org/10.1152/ajplung.00300.2014

Manibusan, M.K., Odin, M., Eastmond, D.A., 2007. Postulated carbon tetrachloride mode of action: a review. J. Environ. Sci. Health C. Environ. Carcinog. Ecotoxicol. Rev. 25(3), 185-209. http://dx.doi.org/10.1080/10590500701569398

Mannaerts, I., Leite, S.B., Verhulst, S., Claerhout, S., Eysackers, N., Thoen, L.F., Hoorens, A., Reynaert, H., Halder, G., van Grunsven, L.A., 2015. The Hippo pathway effector YAP controls mouse hepatic stellate cell activation. J. Hepatol. 63(3), 679-88. http://dx.doi.org/10.1016/j.jhep.2015.04.011

Meng, Z., Moroishi, T., Guan, K.L., 2016. Mechanisms of Hippo pathway regulation. Genes Dev. 30(1), 1-17. http://dx.doi.org/10.1101/gad.274027.115

Moustakas, A., Heldin, C.H., 2009. The regulation of TGFbeta signal transduction. Development 136(22), 3699-714. http://dx.doi.org/10.1242/dev.030338

Nishio, M., Sugimachi, K., Goto, H., Wang, J., Morikawa, T., Miyachi, Y., Takano, Y., Hikasa, H., Itoh, T., Suzuki, S.O., Kurihara, H., Aishima, S., Leask, A., Sasaki, T., Nakano, T., Nishina, H., Nishikawa, Y., Sekido, Y., Nakao, K., Shin-Ya, K., Mimori, K., Suzuki, A.1., 2016. Dysregulated YAP1/TAZ and TGF-β signaling mediate hepatocarcinogenesis in Mob1a/1b-deficient mice. Proc. Natl. Acad. Sci. U.S.A. 113(1), E71-80. http://dx.doi.org/10.1073/pnas.1517188113

Park, S.M., Ki, S.H., Han, N.R., Cho, I.J., Ku, S.K., Kim, S.C., Zhao, R.J., Kim, Y.W. 2015. Tacrine, an oral acetylcholinesterase inhibitor, induced hepatic oxidative damage, which was blocked by liquiritigenin through GSK3-beta inhibition. Biol. Pharm. Bull. 38(2), 184-192. http://dx.doi.org/10.1248/bpb.b14-0043

Perumal, N., Perumal, M., Halagowder, D., Sivasithamparam, N., 2017. Morin attenuates diethylnitrosamine-induced rat liver fibrosis and hepatic stellate cell activation by co-

ordinated regulation of Hippo/Yap and TGF-β1/Smad signaling. Biochimie. 140, 10-19. http://dx.doi.org/10.1016/j.biochi.2017.05.017

Puche, J.E., Saiman, Y., Friedman, S.L., 2013. Hepatic stellate cells and liver fibrosis. Compr. Physiol. 3(4), 1473-92. http://dx.doi.org/10.1002/cphy.c120035

Ramachandran, P., Iredale, J.P., 2012. Liver fibrosis: a bidirectional model of fibrogenesis and resolution. Q. J. M. 105(9), 813-7. http://dx.doi.org/10.1093/qjmed/hcs069

Sakurai, T., Kudo, M., 2013. Molecular link between liver fibrosis and hepatocellular carcinoma. Liver Cancer 2(3-4), 365-6. http://dx.doi.org/10.1159/000343851

Sánchez-Valle, V., Chávez-Tapia, N.C., Uribe, M., Méndez-Sánchez, N., 2012. Role of oxidative stress and molecular changes in liver fibrosis: a review. Curr. Med. Chem. 19(28), 4850-60.

Seki, E., Schwabe, R.F., 2015. Hepatic inflammation and fibrosis: functional links and key pathways. Hepatology 61(3), 1066-79. http://dx.doi.org/10.1002/hep.27332

Varelas, X., Samavarchi-Tehrani, P., Narimatsu, M., Weiss, A., Cockburn, K., Larsen, B.G., Rossant, J., Wrana, J.L., 2010. The Crumbs complex couples cell density sensing to Hippo-dependent control of the TGF-β-SMAD pathway. Dev. Cell 19(6), 831-44. http://dx.doi.org/10.1016/j.devcel.2010.11.012

Wang, D., Wong, H.K., Feng, Y.B., Zhang, Z., 2014. Liquiritigenin exhibits antitumour action in pituitary adenoma cells via Ras/ERKs and ROS-dependent mitochondrial signalling pathways. J. Pharm. Pharmacol. 66(3), 408-17. http://dx.doi.org/10.1111/jphp.12170

Xin, M., Kim, Y., Sutherland, L.B., Murakami, M., Qi, X., McAnally, J., Porrello, E.R., Mahmoud, A.I., Tan, W., Shelton, J.M., Richardson, J.A., Sadek, H.A., Bassel-Duby, R., Olson, E.N., 2013. Hippo pathway effector Yap promotes cardiac regeneration. Proc.

Natl. Acad. Sci. U.S.A. 110(34), 13839-44. http://dx.doi.org/10.1073/pnas.1313192110

Yazdani, S., Bansal, R., Prakash, J., 2017. Drug targeting to myofibroblasts: Implications for fibrosis and cancer. Adv. Drug Deliv. Rev. 121, 101-116. http://dx.doi.org/10.1016/j.addr.2017.07.010

Zhang, Y., He, Y., Yu, H., Ma, F., Wu, J., Zhang, X., 2015. Liquiritigenin Protects Rats from Carbon Tetrachloride Induced Hepatic Injury through PGC-1α Pathway. Evid. Based Complement. Alternat. Med. 2015, 649568. http://dx.doi.org/10.1155/2015/649568

Zhao, B., Ye, X., Yu, J., Li, L., Li, W., Li, S., Yu, J., Lin, J. D., Wang, C.Y., Chinnaiyan, A.M., Lai, Z.C., Guan, K.L., 2008. TEAD mediates YAP-dependent gene induction and growth control. Genes Dev. 22(14), 1962-71. http://dx.doi.org/10.1101/gad.1664408

Zhubanchaliyev, A., Temirbekuly, A., Kongrtay, K., Wanshura, L.C., Kunz, J., 2016. Targeting mechanotransduction at the transcriptional Level: YAP and BRD4 are novel therapeutic targets for the reversal of liver fibrosis. Front. Pharmacol. 7, 462. http://dx.doi.org/10.3389/fphar.2016.00462

Figure Legends

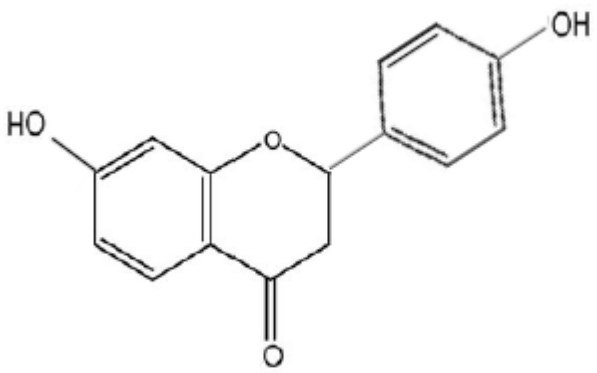

Fig. 1. The chemical structure of liquiritigenin (LQ).

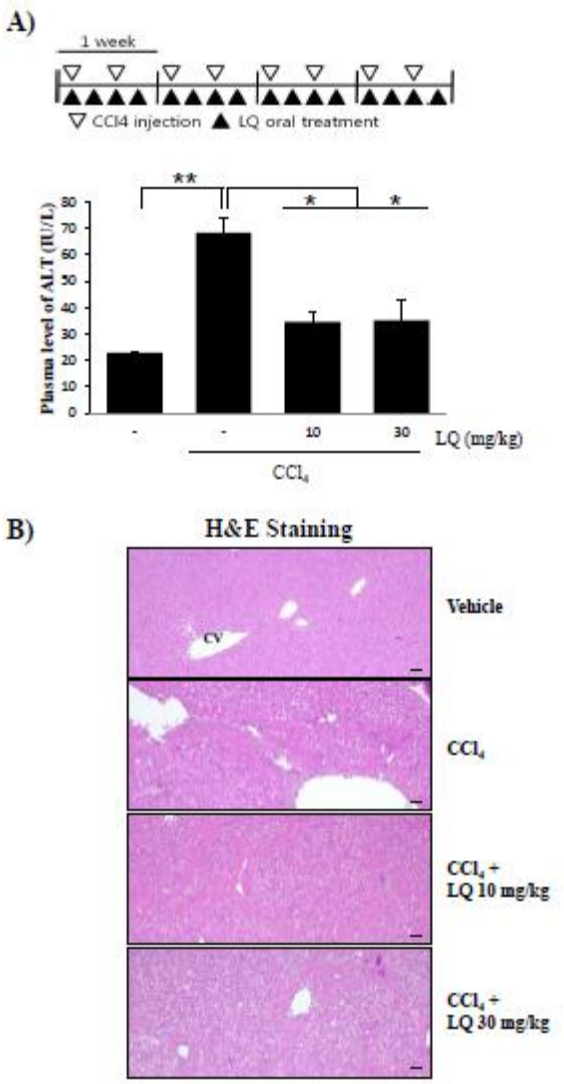

Fig. 2. The effect of LQ on CCl_4-induced liver toxicity in mice. Mice were injected with CCl_4 (0.5 ml/kg) intraperitoneally twice a week and administered LQ (10 or 30 mg/kg) orally four times per week for 4 weeks. After treatment, (A) the activities ALT were assayed by using semi-automated blood chemistry analyzer. Data represents the mean ± SD. * *P* < *0.05;* ** *P* < *0.01*. (B) Representative histological sections of the liver. The liver sections from left lateral lobes were stained with haematoxylin and eosin (H&E) in mice treated with vehicle, CCl_4, CCl_4 + LQ 10 mg/kg, and CCl_4 + LQ 30 mg/kg. Scale bars = 80 μm.

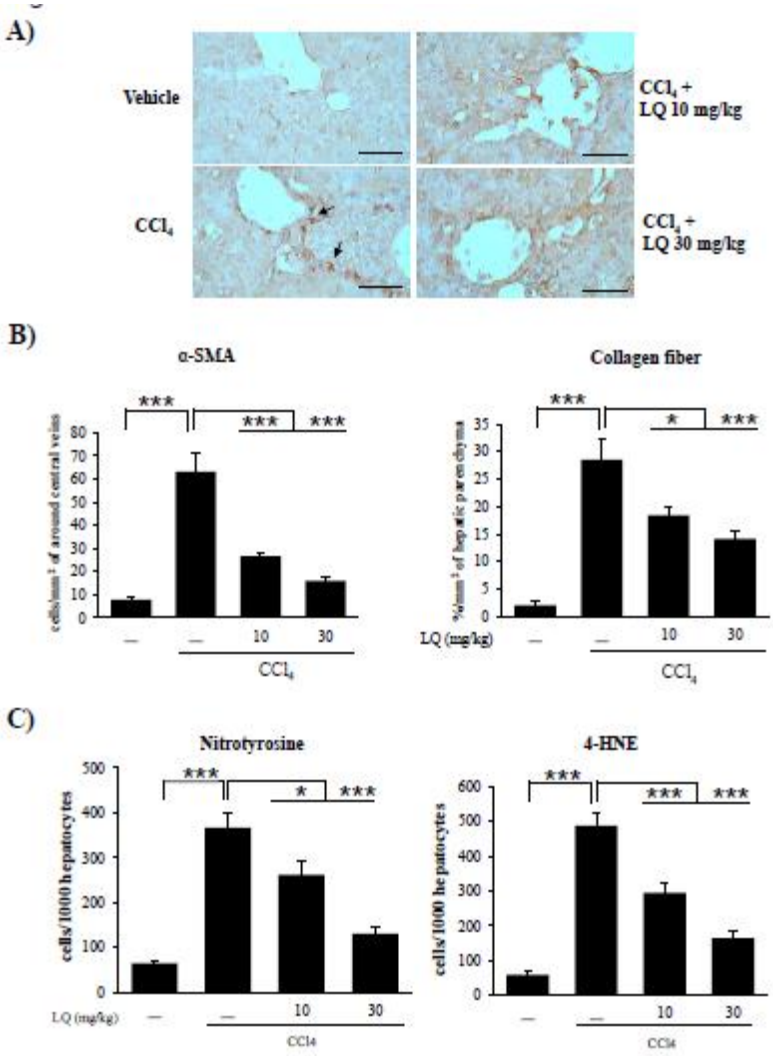

Fig. 3. Effects of LQ on liver fibrosis induced by CCl_4. (A) Liver fibrosis was observed by immunohistochemical staining of α-SMA-positive cells. Scale bars = 80 μm. (B) Quantitation of α-SMA-positive cells (left) and collagen fiber occupied regions (right). Data represents the mean ± SD from seven separate experiments. * *P < 0.05; *** P < 0.001*. (C) Quantitation of nitrotyrosine (left) and 4-HNE positive cells (right). Data represents the mean ± SD from seven separate experiments. * *P < 0.05; *** P < 0.001*.

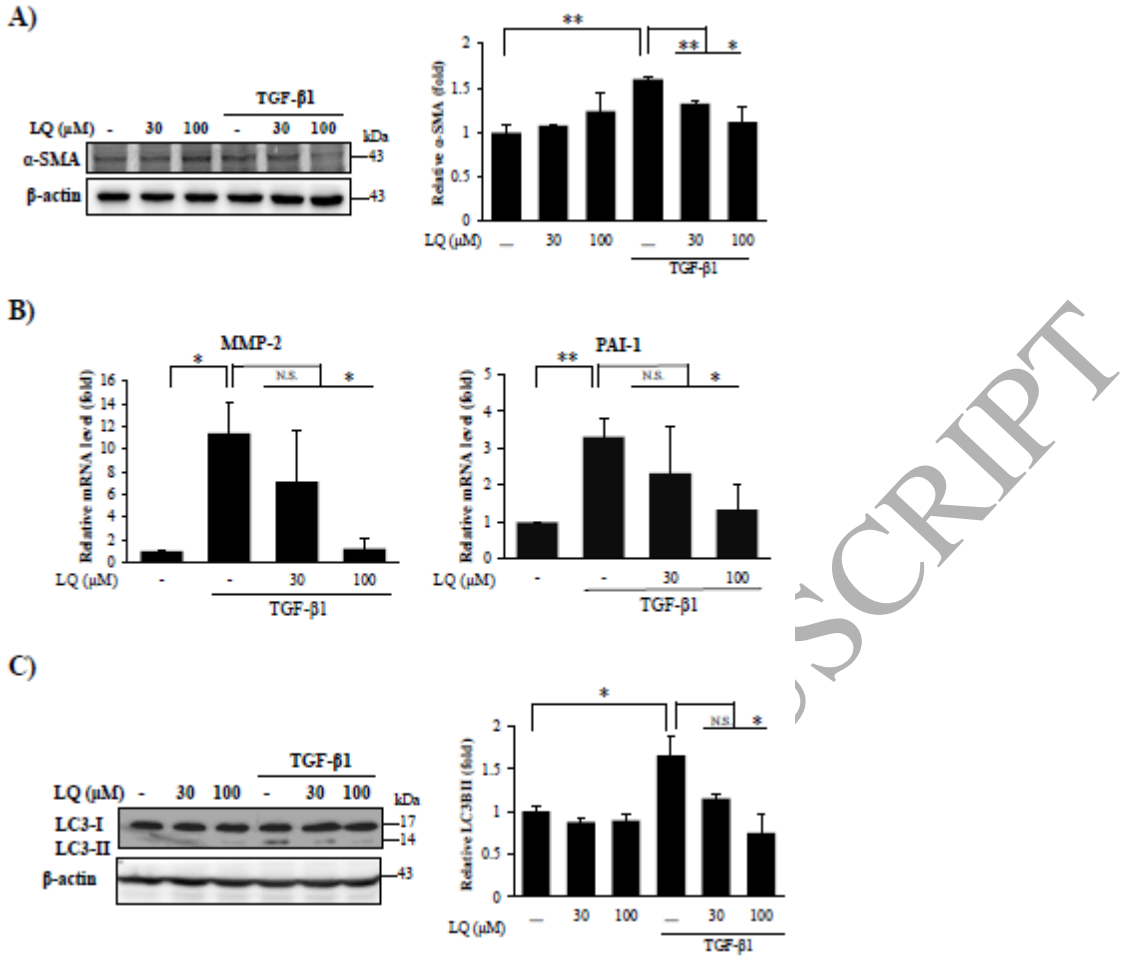

Fig. 4. Effects of LQ on TGF-β1-induced HSCs activation. (A) LQ suppresses TGF-β1-induced expression of the myofibroblast marker protein α-SMA. Western blot analyses were performed on the lysates of serum starved LX-2 cells that were treated with LQ in the presence or absence of TGF-β1 (5 ng/ml) for an additional 24 h. β-actin served as a loading control. Protein levels were presented as relative band intensities to control (vehicle treated) group. (B) Real-time PCR was assessed to investigate mRNA level of PAI-1 and MMP-2, TGF-β1 target genes. (C) LQ suppresses TGF-β1-induced expression of the autophagy related proteins, LC3II. Data represents the mean ± SD from three separate experiments. * *P* *< 0.05; **P < 0.01.*

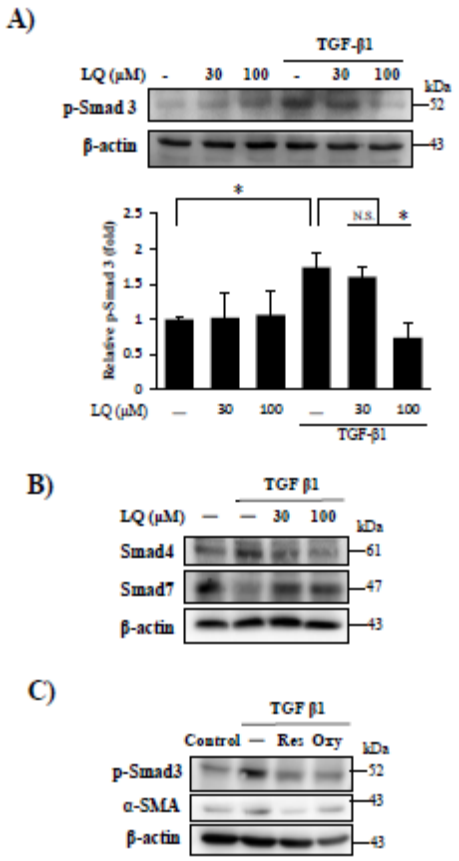

Fig. 5. Effects of LQ on TGF-β1/Smad pathway in HSCs. LQ suppresses the activation of TGF-β1/Smad pathway. (A) Phosphorylation levels of Smad 3 were analyzed by immunoblotting with specific antibodies. Western blot performed on the lysates of serum starved LX-2 cells that were treated with LQ in the presence or absence of TGF-β1 (5 ng/ml) for an additional 24 h. β-actin served as a loading control. Protein levels were presented as relative band intensities to control (vehicle treated) group. (B) Protein expression levels of different Smads subtypes (pSmad3, Smad4, and Smad7) were analyzed using western blot. (3) Effects of resveratrol (Res) and oxyresveratrol (OXY) on TGF-β1-stimulated phosphorylation of Smad 3. The cells were treated with 30 μM of the compounds for 1 h and then with TGF-β1 (5 ng/ml, 24 h).

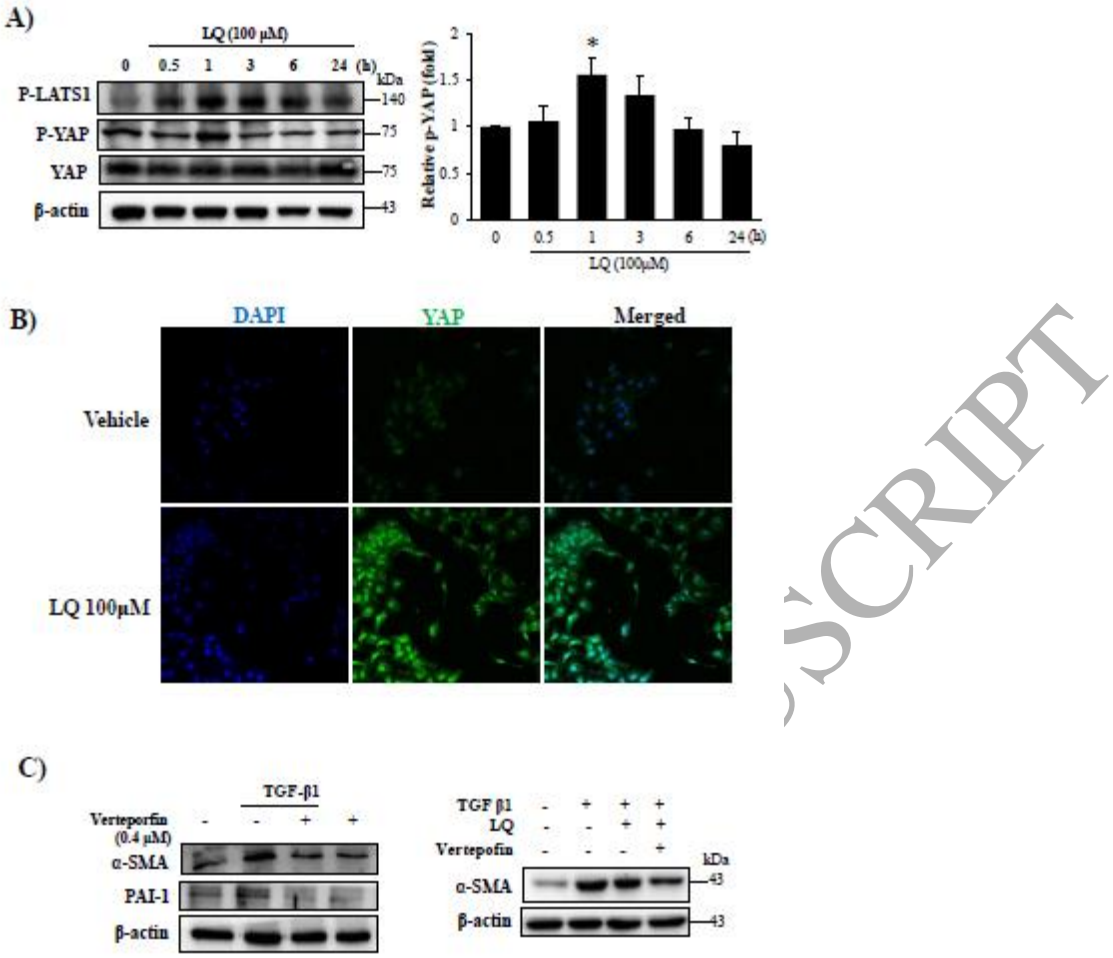

Fig. 6. Effects of LQ on Hippo signaling. LQ induced phosphorylation of the proteins associated with Hippo pathway, LAST and YAP. (A) Western blot analyses were performed with the lysates of cells that had been treated with 100 μM LQ for the indicated time period. β-actin was used to serve as a loading control. Protein levels were presented as relative band intensities to control group. Results were represented as the mean ± S.D. calculated from three independent trials. * $P < 0.05$. (B) The pictures of the fluorescence micrographs show the induction of YAP resulting from the treatment of LQ in LX-2 cells. Cells were treated with 100 μM LQ for 1hr and were stained Yap with FITC labelled secondary anti-rabbit antibody. (C) Verteporfin inhibited HSCs activation by TGF-β1` (left). LQ and verteporfin

combination synergically suppressed TGF-β1-induced expression of α-SMA (right). Western blot analysis of α-SMA and PAI-1 were performed with lysates of LX-2 cells that had been pretreated with 400 nM verteporfin and/or 100 μM LQ for 1 h being followed by exposure to TGF-β1 (5 ng/ml) for 24 h.

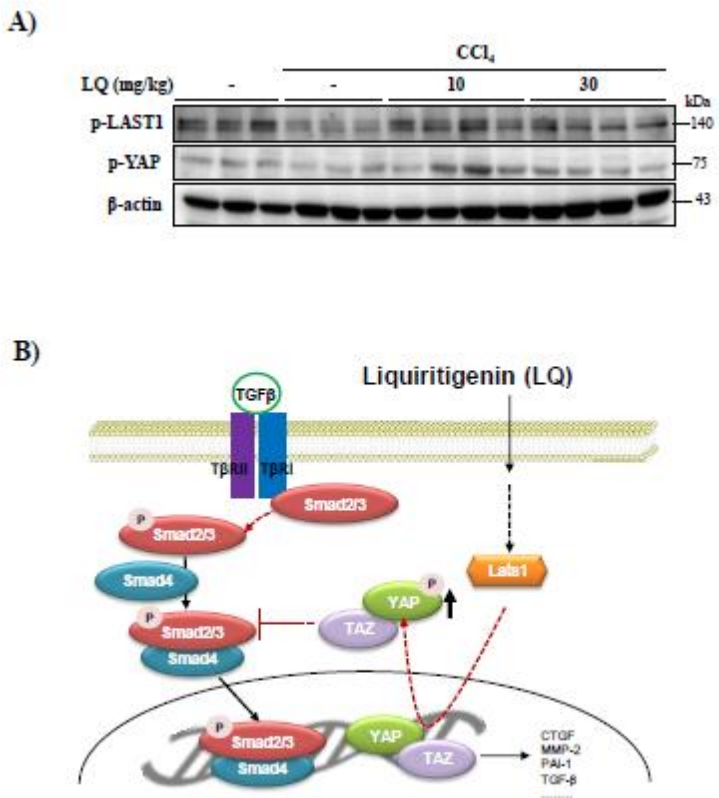

Fig. 7. (A) Western blot analyses were assessed with homogenates of liver tissues in mice treated with vehicle, CCl_4, CCl_4 + LQ 10 mg/kg, and CCl_4 + LQ 30 mg/kg groups. (B) Schematic diagram showed that LQ regulated of Hippo/Yap and TGF-β1/Smad signaling pathway ameliorating liver fibrosis and hepatic stellate cell activation.

Table 1. Primers used in realtime PCR in this study.

Human gene	Sense	Antisense
MMP-2	5′-CACCAGCCAGAAGTGACAGA-3′	5′-ATGTGCCTGCGTGTATGTGT-3′
PAI-1	5′-CGCCAGAGCAGGACGAA-3′	5′-CATCTGCATCCTGAAGTTCTCA-3′
GAPDH	5′-AACGACCCCTTCATTGAC-3′	5′-TCCACGACATACTCAGCAC-3′

Table 2. General histomorphometrical analysis of liver in CCl_4-treated mice livers.

Index / groups	Numbers of inflammatory cells infiltrated (cells/mm^2 of hepatic parenchyma)	Numbers of degenerative hepatocytes (cells/1000 hepatocytes)
Controls	6.00 ± 2.71	7.57 ± 3.99
CCl_4	141.86 ± 34.96[a]	178.00 ± 52.34[a]
CCl_4 + LQ 10 mg/kg	96.29 ± 37.54[ac]	104.00 ± 45.10[ac]
CCl_4 + LQ 30 mg/kg	50.29 ± 18.65[ab]	50.29 ± 19.50[ab]

Values are expressed as mean ± SD of seven mice

[a] $P < 0.01$ as compared with intact control by Mann-Whitney U test

[b] $P < 0.01$ and [c] $P < 0.05$ as compared with CCl_4 control by Mann-Whitney U test

Graphical Abstract